Supporting Information

Metal-metal bonded pentamolybdate hybrids as electron storage material

Meng Cao,[a,b] Jie Zi,[b] Ruili Sang*[b] and Li Xu*[b,c]

[a]College of Chemistry and Materials Science, Fujian Normal University, Fuzhou, Fujian 350007, China.

[b]State Key Laboratory of Structural Chemistry, Fujian Institute of Research on the Structure of Matter, Chinese Academy of Sciences, Fuzhou, Fujian, 350002, China.

[c]Fujian College, University of Chinese Academy of Science, Fuzhou, Fujian, 350002, China.

E-mail: xli@fjirsm.ac.cn

Contents

1. Materials and Syntheses

Materials: All chemical reagents and drugs were purchased directly for use without further isolation and purification. The precursors $[Mo_3O_2(O_2CCH_3)_6(H_2O)_3]ZnCl_4\cdot 8H_2O$ was prepared according to the literature methode.[1-3]

Preparation of 2D-$[Mo^{IV}_3Mo^{VI}_2O_{10}Sr_2(H_2O)_5(C_6H_4O_7)_2py_3]\cdot 3.5H_2O$ (1):

A mixture of $[Mo_3O_2(O_2CCH_3)_6(H_2O)_3]ZnCl_4\cdot 8H_2O$ precursors (0.1 g, 0.1 mmol), $SrCO_3$ (0.015 g, 0.10 mmol), citric acid ($C_6H_8O_7$) (0.015 g, 0.08 mmol), H_2O (2 ml) and pyridine (8 ml) were sealed in a 20 ml Teflon-lined stainless-steel reactor and heated to 393 K for three days. Then the reactor was cooled to room temperature at 2 K/h to produce yellow flake crystals of **1**. (>40% yield based on Mo). Anal. Calc. for $C_{27}H_{40}Mo_5N_3O_{32.5}Sr_2$ (Mr.=1581.56): C, 20.50%; H, 2.55%; N, 2.65%; Sr, 11.08%; Mo, 30.33%; Found: C, 21.04%; H, 2.63%; N, 2.81%; Sr, 9.7%; Mo, 28.40%. IR (KBr, cm^{-1}): 3472 (m, O-H, N-H), 1641-1606 (s, O-H, N-H), 1404 (s, C-H), 1067-1222 (w, C-N, C-C), 926 (m, Mo=O_t), 733-873 (s, Mo–O_b–Mo), 643 (w, Mo–O_b–Mo). CCDC No. 2261568.

Preparation of 1D-$[Mo^{IV}_3Mo^{VI}_2O_{10}Sr(H_2O)_3(C_6H_4O_7)_2py_3]\cdot py\cdot 2[NH_2(CH_3)_2]\cdot 2H_2O$ (2):

A mixture of $[Mo_3O_2(O_2CCH_3)_6(H_2O)_3]ZnCl_4\cdot 8H_2O$ precursors (0.1 g, 0.1 mmol), $SrCO_3$ (0.015 g, 0.10 mmol) , citric acid ($C_6H_8O_7$) (0.015 g, 0.08 mmol), H_2O (1 ml), DMF (0.5 ml) and pyridine (9 ml) were sealed in a 20 ml Teflon-lined stainless-steel reactor and heated to 393 K for two days. Then the reactor was cooled to room temperature at 2 K/h to produce yellow block crystals of **2**. (>40% yield based on Mo) Anal. Calc. for $C_{36}H_{54}Mo_5N_6O_{29}Sr$ (Mr.=1602.17): C, 27.12%; H, 2.91%; N, 5.27%; Sr, 5.50%; Mo, 30.09%; Found: C, 25.96%; H, 3.26%; N, 4.61%; Sr, 5.30%; Mo, 30.24%. IR (KBr, cm^{-1}): 3449 (s, O-H, N-H), 1635 (s, O-H, N-H), 1401 (s, C-H), 1067-1220 (w, C-N, C-C), 917 (m, Mo=O_t), 725-882 (s, Mo–O_b–Mo), 643 (w, Mo–O_b–Mo). CCDC No. 2261583.

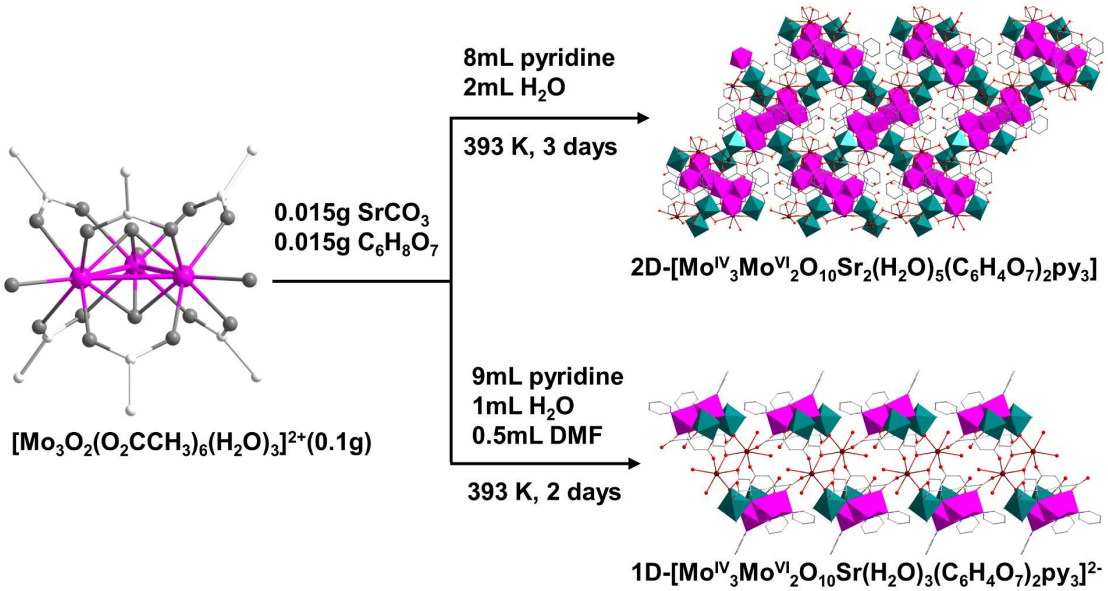

Scheme 1. Synthesis of the hybrid-POM**1** and hybrid-POM**2** through the solvothermal oxidation aggregation of $[Mo_3O_2(O_2CCH_3)_6(H_2O)_3]ZnCl_4$ at different reaction conditions.

2. Instruments and Physical Measurements

General information:

Elemental analyses for C, H and N were performed with a vario MICRO elemental analyzer, and inductively coupled plasma photoemission spectroscopy for metals Mo and Sr was performed with an Avio220Max. IR spectra were obtained on a vertex X70 infrared spectrometer using KBr pellets with a measurement range of 4000-400 cm^{-1}. The X-ray photoelectron spectroscopy (XPS) measurements were carried out on an ESCALAB 250Xi spectrometer equipped with an Al Kα-ray source. The C 1s signal (284.8 eV) is used as the reference calibration binding energy. Thermogravimetric analysis (TGA) was performed on the STA449C thermal analyzer under N_2 flow with 10 °C/min heating. Solid UV-visible spectra were collected on a Perkin-Elmer Lamber-950 spectrophotometer in the wavelength range of 200-800 nm. Powder X-ray diffraction (PXRD) was performed on a Miniflex 600 powder diffraction instrument.

Single-crystal X-ray structure analysis:

Single crystal X-ray diffraction data of **1** and **2** were recorded on a Bruker D8-venture diffractometer (λ (Mo *K*α) = 0.71073 Å) at low temperature (170K/150K) equipped with a graphite monochromator. All absorption corrections were performed using multi-scan. The structures were solved by direct methods and refined by full-matrix least-squares on F^2 with the SHELXTL-2016 program package.[4] The CCDC No. 2261568 (for **1**) and CCDC No. 2261583 (for **2**) contains the supplementary crystallographic data for this paper. These data can be obtained free of charge from The Cambridge Crystallographic Data Centre via www.ccdc.cam.ac.uk/data_request/cif.

Electrochemical measurements:

The collected crystalline samples were dried at 130 °C under argon flow for 12 hours to remove lattice water molecules. The cathode material was prepared by dispersing adequately dried active material (**1** and **2**), acetylene black and poly (vinyl difluoride) (PVDF) binder with a weight ratio of 3:5:2 in a suitable amount of solvent of N-methyl-2-pyrroldone (NMP) to form homogeneous slurries under vigorous stir, then pasting onto aluminum foil. The obtained cathodes were dry at the temperature of 105 °C under vacuum for 12 hours. The mass loading of the active material on the Al foil is about 0.3-0.4 mg. Such a cathode round piece (radius=7 mm), a celgard 2500 separator, a lithium foil as anode and the electrolyte of 1M $LiPF_6$ in ethylene carbonate (EC)/diethyl carbonate (DEC) (1:1, v/v), were sealed into a CR2032-type coin cell, in an argon-filled glovebox. Galvanostatic charge/discharge measurements were performed on a Neware Battery testing system (CT-4008Tn, Shengzhen, China) at different current densities in the voltage range of 1.5-4.0 V (vs. Li/Li^+). Cyclic voltammetry (CV) curves were obtained with the CHI 660e electrochemical workstation (Shanghai, China). Electrochemical impedance spectroscopy (EIS) was performed on the CHI 660e electrochemical workstation (Shanghai, China).

Conductivity measurement:

The electrical conductivity measurement method in this work is referenced to the published paper.[5] The testing thin pellets samples were prepared by vacuum drying the powder samples at 90 °C for 12 hours and then die-pressing powder samples (about 3-5 mg) with a pressure of 10 MPa. The obtained thin pellets samples, with a diameter of 2.5 mm and a thickness of about 1.0 mm, and then were coated with conductive silver on both sides and electrical contacts were made using gold wires. The prepared samples were dried at 60 °C under vacuum for 10 hours and then the electrical conductivity measurement was conducted. The conductivity of the thin sample particle is measured with the KEITHLEY 4200-SCS semiconductor parameter analyzer using the

DC two-terminal method. The bulk electrical conductivity of **1** and **2** was calculated by the following equation.

$$\sigma = \frac{l \times G}{S}$$

Where σ is electrical conductivity of the sample (S cm^{-1}), l is thickness of sample (cm), S is contact area (cm^2), and G is the conductance obtained from the current versus voltage curves.

Details of Theoretical calculation:

First-principles density functional theory (DFT)[6] calculations were performed using the GAUSSIAN16 package[7] at the B3LYP/Lanl2DZ[8] level for structure of **1**, **2** and $[Mo_3O_4(C_2O_4)_3(Mepy)_3]^{2-}$. The Lanl2DZ[9] pseudopotential were used for Mo and Sr metal atoms, the 6-31*G[10] basis set for the rest of the atoms (C, H, O and N). In all the calculations, a closed-shell singlet state was assumed and spin-restricted MOs was used.

3. Crystallographic data

Table S1. X-ray crystallographic data for **1** and **2**.

Compound	**1**	**2**
Empirical formula	$C_{27}H_{40}Mo_5N_3O_{32.5}Sr_2$	$C_{36}H_{54}Mo_5N_6O_{29}Sr$
Formula weight	1581.56	1602.17
Temperature	170(2) K	150(2) K
Wavelength	0.71073 Å	0.71073 Å
Crystal system	Monoclinic	Triclinic
Space group	$P2_1/c$	$P\bar{1}$
Unit cell dimensions	a = 16.1134(16) Å b = 15.6367(11) Å c = 18.9562(17) Å α= 90° β=106.944(4)° γ = 90°	a = 10.6907(6) Å b = 15.5420(11) Å c = 17.3408(11) Å α= 67.740(2)° β= 79.773(2)° γ =80.703(3)°
Volume	4568.9(7) $Å^3$	2610.1(3) $Å^3$
Z	4	2
Density (calculated)	2.299 g/cm^3	2.039 g/cm^3
Absorption coefficient	3.752 mm^{-1}	2.276 mm^{-1}
F(000)	3076	1584
θ range	2.246 to 25.719°.	2.180 to 27.536°.
Index ranges	-19 19, -19 19, -23 23	-13 13, -20 19, -22 21
Reflections collected	40951	32233
Independent reflections	8655 [R(int) = 0.0797]	11925 [R(int) = 0.0394]
Completeness	99.8 %	99.3 %
Refinement method	Full-matrix least-squares on F^2	Full-matrix least-squares on F^2
restraints / parameters	7 / 631	63 / 689
Goodness-of-fit on F^2	1.028	0.997
Final R indices [I>2σ(I)]	R1 = 0.0375, wR2 = 0.0954	R1 = 0.0409, wR2 = 0.1040
R indices (all data)	R1 = 0.0464, wR2 = 0.1014	R1 = 0.0496, wR2 = 0.1103

$R_1=\sum||F_o|-|F_c||/\sum|F_o|$; $wR_2=\{\sum[w(F_o^2-F_c^2)^2]/\sum[w(F_o^2)^2]\}^{1/2}$

4. Molecular and crystal structures

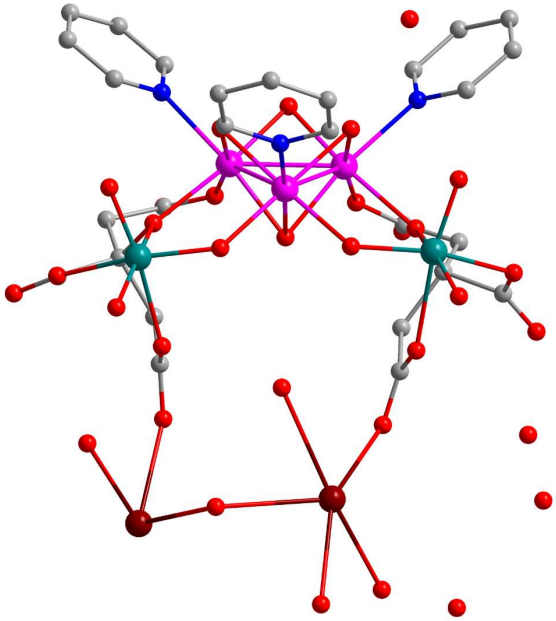

Figure S1. View of the asymmetric unit of **1**, all hydrogen atoms are omitted for clarity.

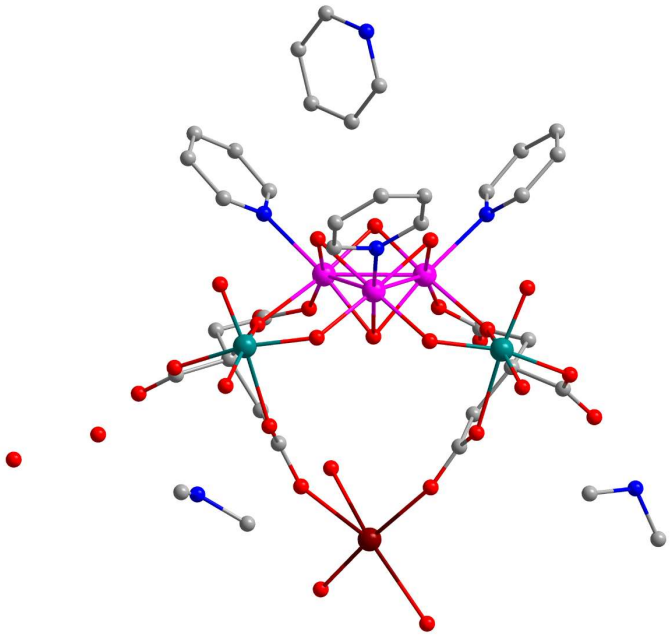

Figure S2. View of the asymmetric unit of **2**, all hydrogen atoms are omitted for clarity.

.

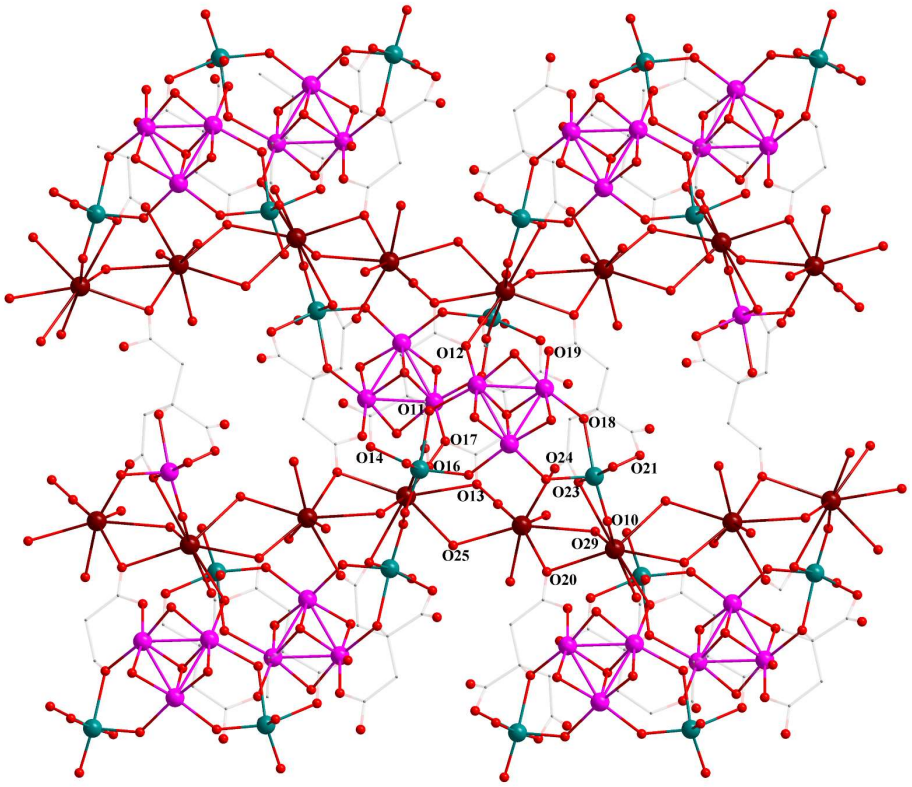

Figure S3. Schematic representation of the formation of the two-dimensional structure of **1**. Color code: Mo^{IV}, pink; Mo^{VI}, teal; Sr, dark red; N, blue; O, red; C, gray (pyridine six-membered rings are omitted and citrate ligands made transparent for clarity).

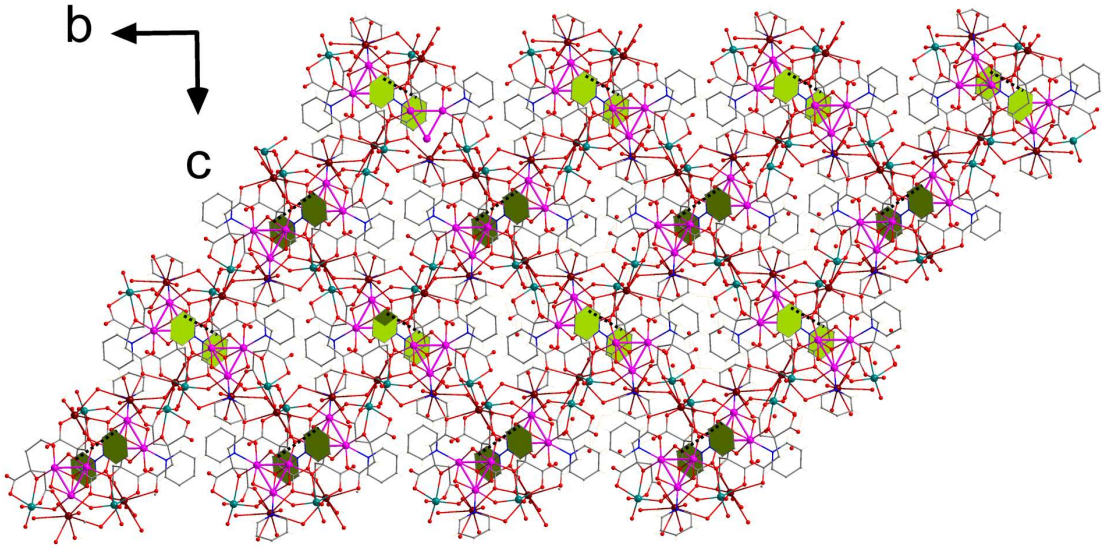

Figure S4. The 3D supramolecular structure of **1** achieved by π slipped stacking interactions between pyridine molecules (six membered rings with green shade). Color code: Mo^{IV}, pink; Mo^{VI}, teal; Sr, dark red; N, blue; O, red; C, gray.

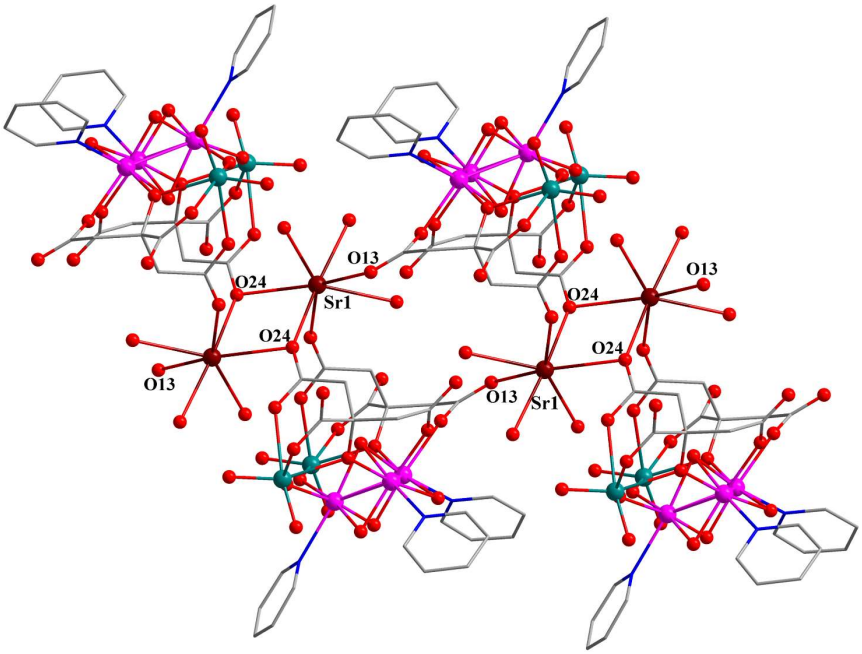

Figure S5. Schematic representation of the formation of the one-dimensional structure of **2**. Color code: Mo^{IV}, pink; Mo^{VI}, teal; Sr, dark red; N, blue; O, red; C, gray.

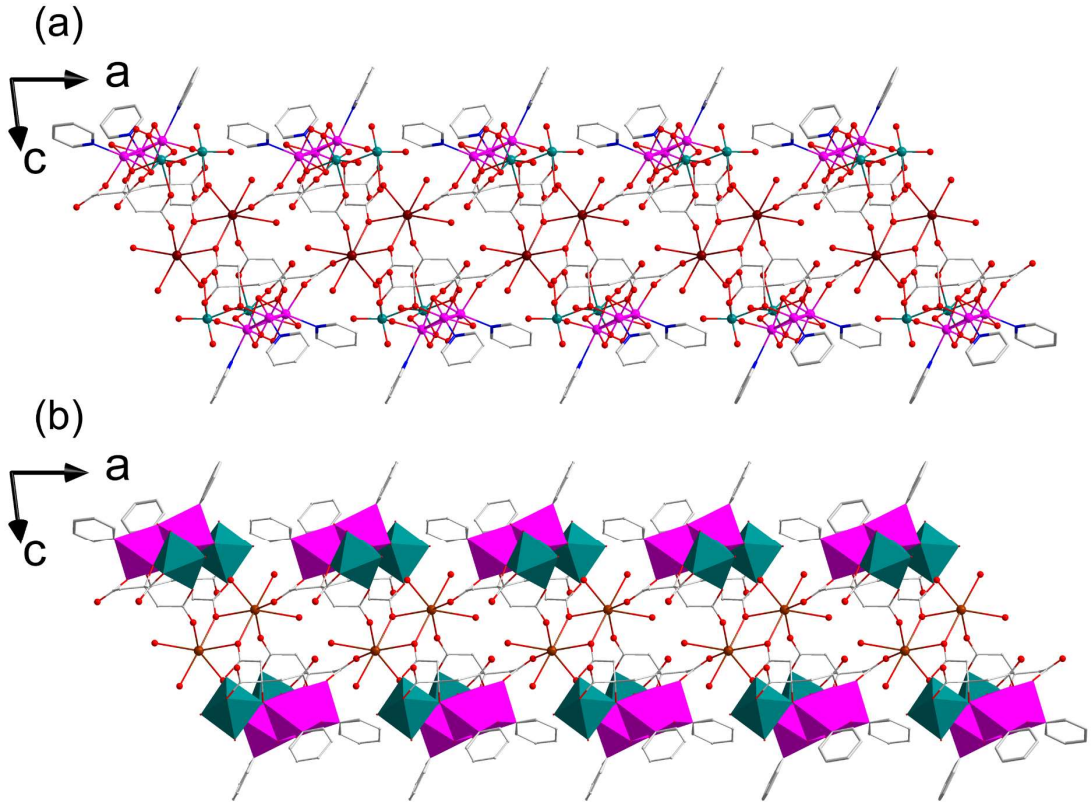

Figure S6. The 1D ball-and-stick structure diagrams (a) and polyhedral structure diagrams (b) of **2** in the ac-plane. Color code: Mo^{IV}, pink; Mo^{VI}, teal; Sr, dark red; N, blue; O, red; C, gray.

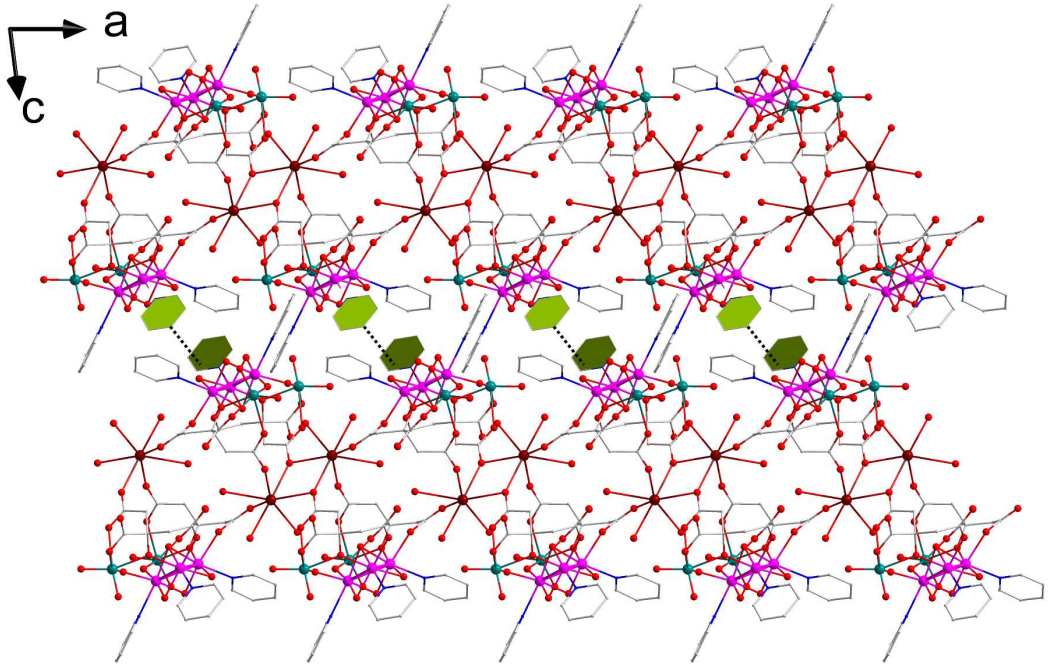

Figure S7. The 2D supramolecular structure diagrams of **2** achieved by slipped π stacking interactions between pyridine molecules (six membered rings with green shade) in the ac plane. Color code: Mo^{IV}, pink; Mo^{VI}, teal; Sr, dark red; N, blue; O, red; C, gray.

5. Band valance sum (BVS) calculations and average bond lengths

Table S2. BVS values of **1**.

1				
Sr1 1.985	O2 2.245	O10 2.032	O18 2.331	O26 0.221
Sr2 2.173	O3 2.176	O11 2.195	O19 2.255	O27 0.219
Mo1 4.201	O4 2.118	O12 2.345	O20 2.185	O28 0.288
Mo2 4.208	O5 2.120	O13 2.147	O21 1.785	O29 0.456
Mo3 4.218	O6 2.019	O14 1.871	O22 1.743	
Mo4 5.928	O7 1.741	O15 1.783	O23 1.776	
Mo5 5.868	O8 2.080	O16 1.670	O24 2.203	
O1 2.084	O9 2.113	O17 2.178	O25 0.399	

Table S3. BVS values of **2**.

2				
Sr1 2.127	O2 2.059	O9 2.210	O16 1.945	O23 1.958
Mo1 4.208	O3 2.132	O10 1.935	O17 2.161	O24 2.221
Mo2 4.158	O4 2.169	O11 2.175	O18 2.215	O25 0.562
Mo3 4.168	O5 2.175	O12 2.101	O19 2.215	O26 0.352
Mo4 5.961	O6 2.147	O13 2.099	O20 1.965	O27 0.298
Mo5 5.905	O7 2.241	O14 1.947	O21 2.188	
O1 2.060	O8 1.860	O15 1.838	O22 1.966	

Table S4. Selected average bond lengths (Å) of **1** and **2**.

Mo^{IV}_3-POMs	d(Mo^{IV}-μ_2O-Mo^{IV})		d(μ_3O-Mo^{IV})	d(Mo^{IV}-μ_2O-Mo^{VI})		d(μ_3O-Mo^{VI})
	d(Mo^{IV}-Mo^{IV})	d(Mo^{IV}-μ_2O)		d(Mo^{IV}-μ_2O)	d(μ_2O-Mo^{VI})	
1	2.498	1.922	2.043	2.040	1.820	2.205
2	2.508	1.924	2.044	2.036	1.831	2.206

6. Spectroscopic characterizations

6.1 TGA

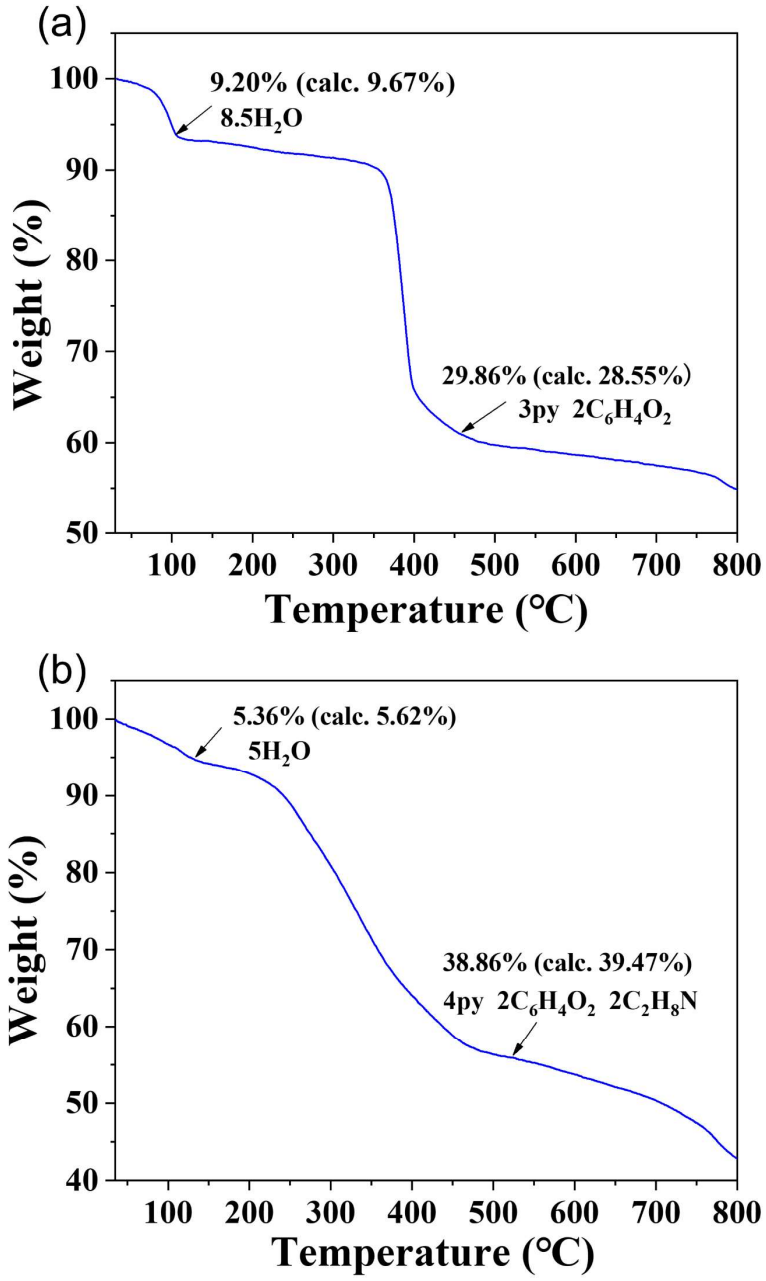

Figure S8. Thermogravimetric analysis curves of **1** (a) and **2** (b).

6.2 IR Spectra

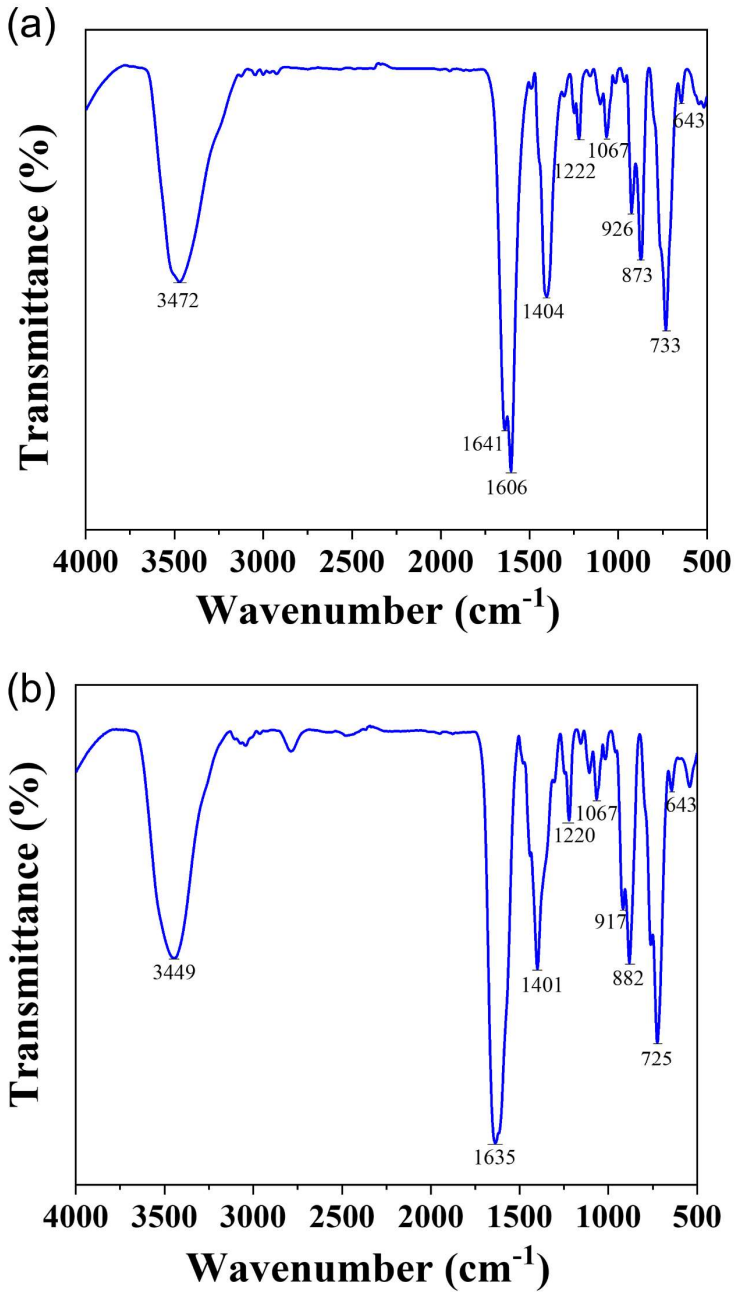

Figure S9. The FT-IR spectra of **1** (a) and **2** (b).

6.3 PXRD

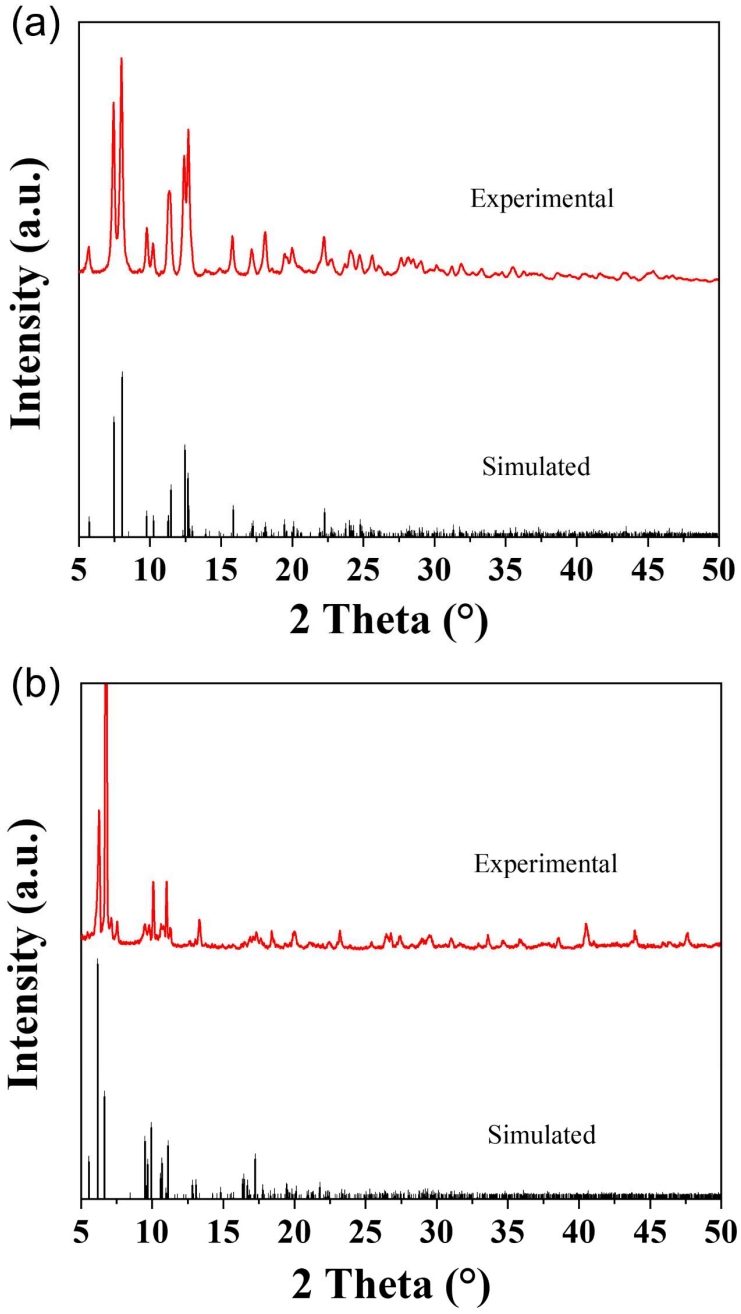

Figure S10. The PXRD patterns of as-prepared (red) crystalline samples and the simulated (black), for **1** (a) and **2** (b).

6.4 XPS

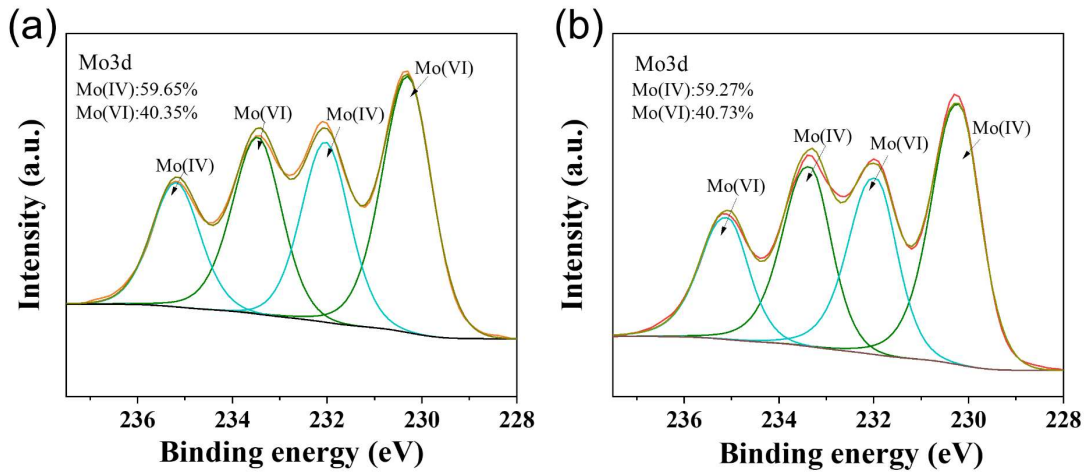

Figure S11. XPS spectra of **1** (a) and **2** (b). (Mo^{IV}:Mo^{VI} = 3: 2).

Table S5. Binding energy (eV) value of **1** and **2**.

	Oxidation state	**Mo $3d_{5/2}$**	**Mo $3d_{3/2}$**
Reported binding	Mo^{IV}-$MoO(OH)_2$	230.2	233.4
energy (eV)	Mo^{VI}-Na_2MoO_4	231.9-232.3	235-235.4
Measured binding	Mo^{IV}	230.30	233.46
energy (eV) of **1**	Mo^{VI}	232.03	235.18
Measured binding	Mo^{IV}	230.22	233.37
energy (eV) of **2**	Mo^{VI}	231.95	235.08

6.5 UV-vis

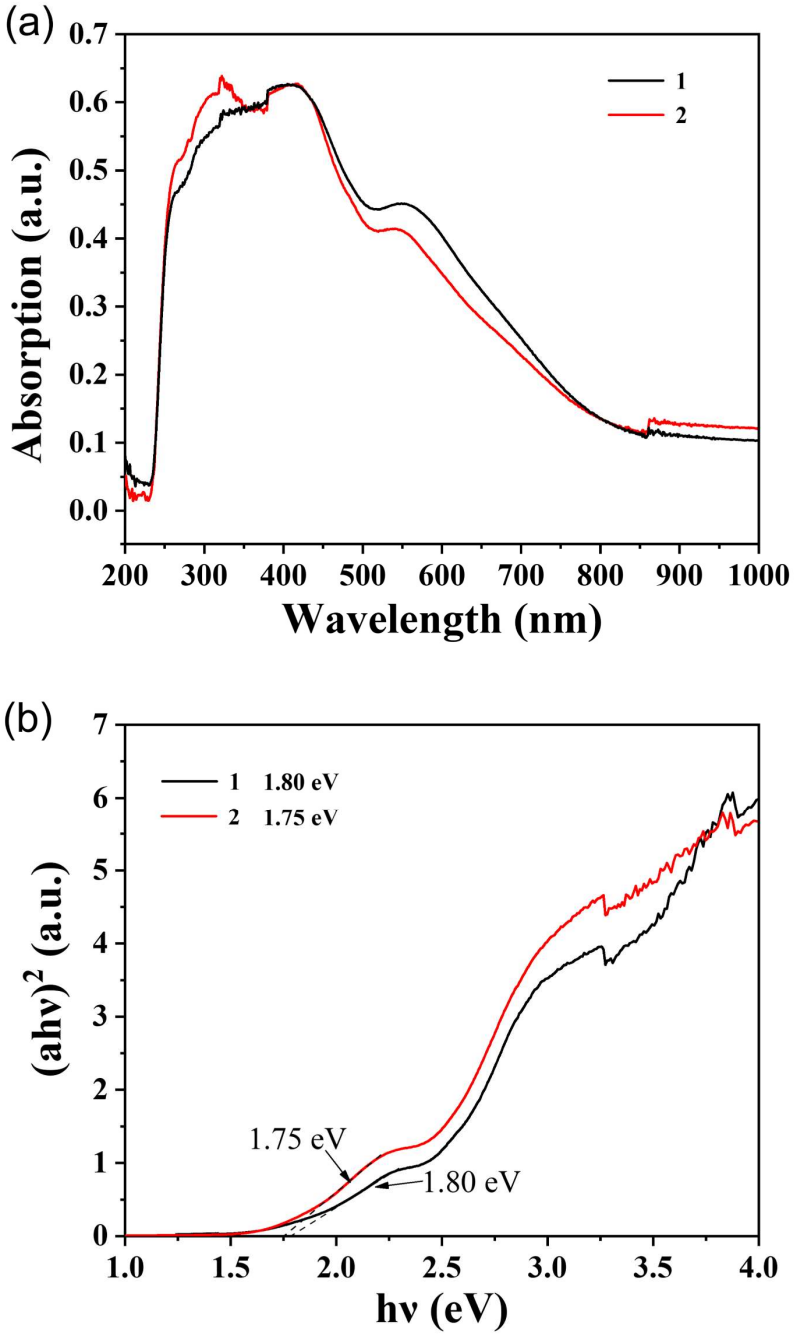

Figure S12. (a) solid-state UV-vis spectra of **1** and **2**. (b) their transformation based on Tauc plot function. The inset indicates the calculated optical band gaps of **1** and **2**.

7. Frontier and metal-metal bonding orbitals

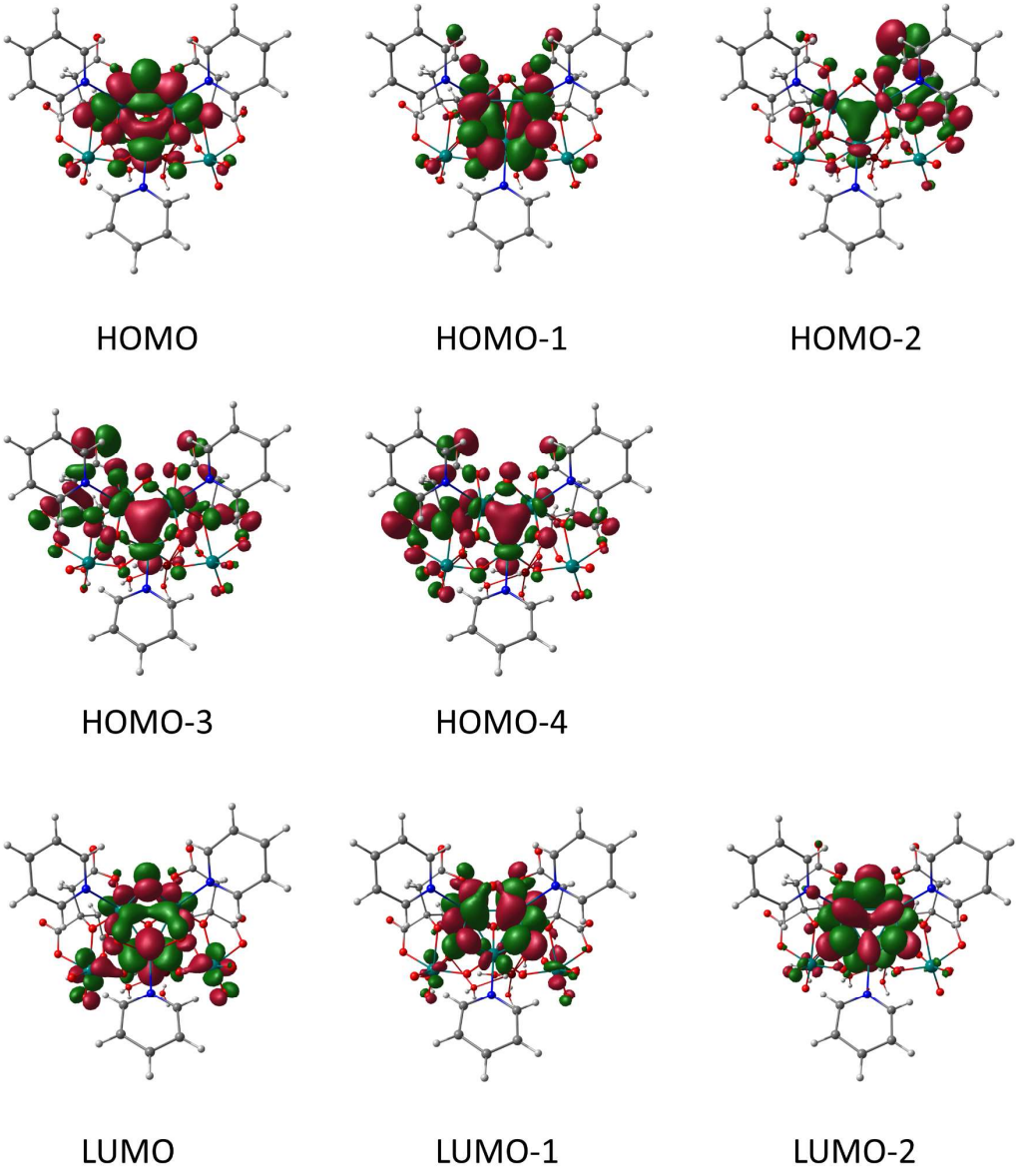

Figure S13. Representative molecular orbitals of **1**.

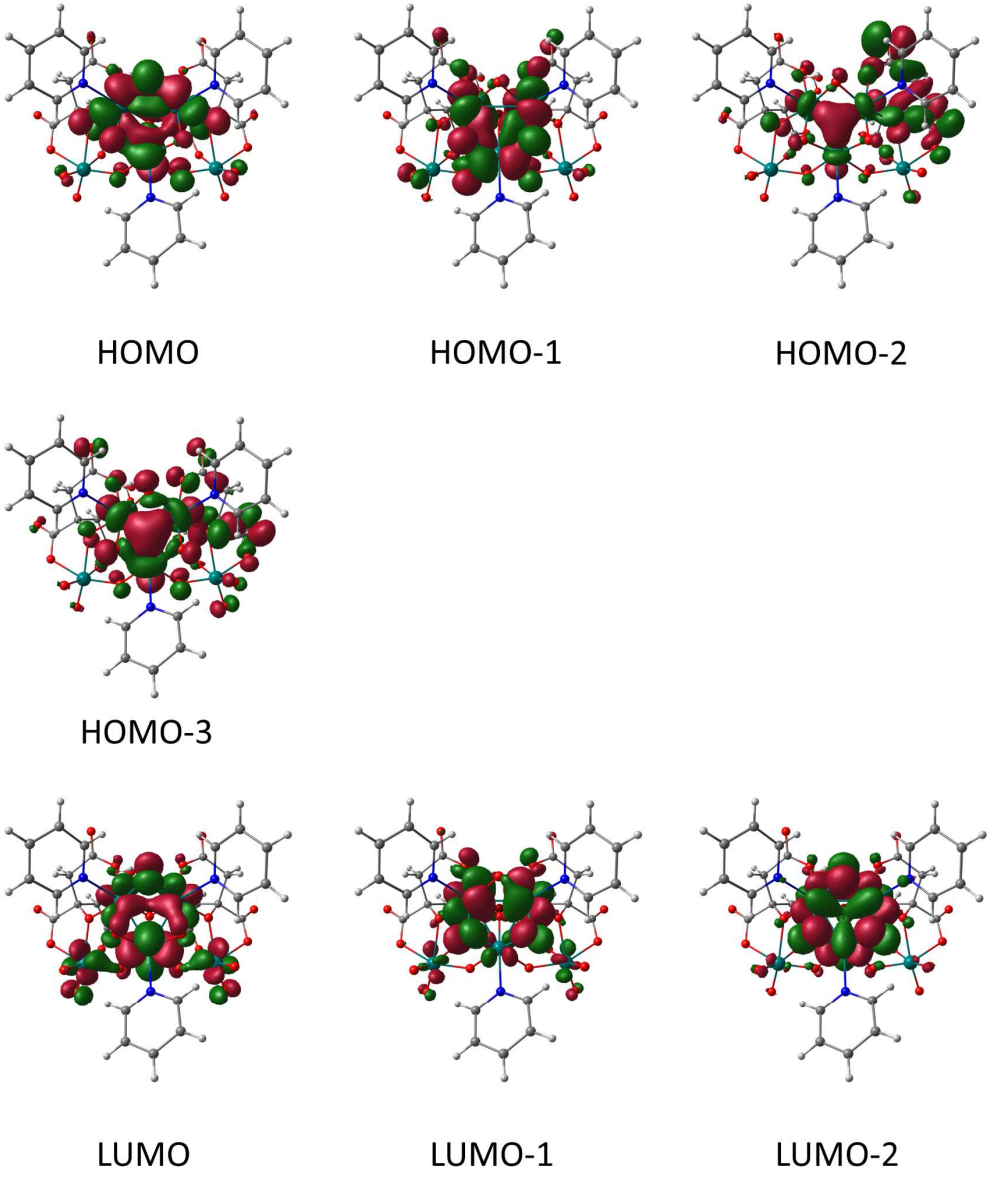

Figure S14. Representative molecular orbitals of **2**.

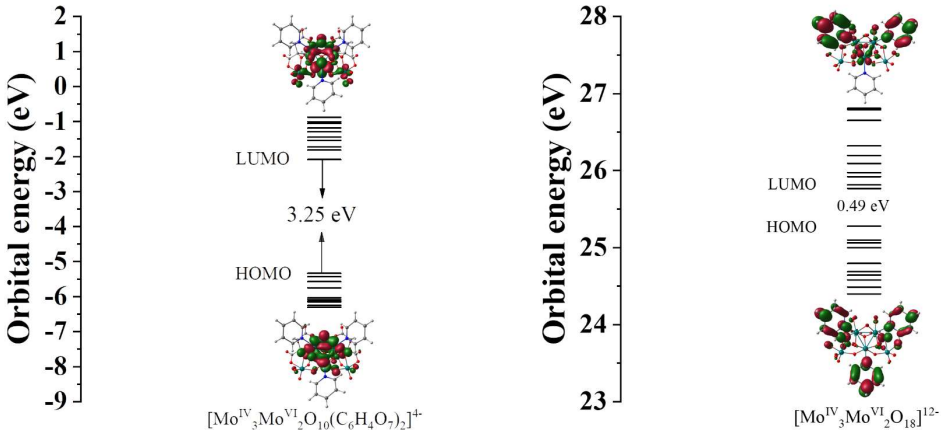

Figure S15. The MO energy levels and HOMO-LUMO gap of $[Mo^{IV}_3Mo^{VI}_2O_{10}(C_6H_4O_7)_2py_3]^{4-}$ and $[Mo^{IV}_3Mo^{VI}_2O_{18}py_3]^{12-}$.

8. Electrochemical characterizations

Table S6. Electric conductivity of **1** and **2** at 25 °C.

Sample	Electric conductivity ($S\ cm^{-1}$)	Electric conductivity ($S\ cm^{-1}$)	
		Sample 1	Sample 2
1	4.73×10^{-10}	3.48×10^{-10}	5.99×10^{-10}
2	1.78×10^{-9}	1.73×10^{-9}	1.83×10^{-9}

Table S7. Comparison of electrochemical performance of reported cathode materials.

Cathode	Specific capacity [$mA\ h\ g^{-1}$]	Rate [C or $mA\ g^{-1}$]	Cycle numbers	Refs.
SiW_{12}	150	50 $mA\ g^{-1}$	20	[11]
SiW_{12}/rGO	275	50 $mA\ g^{-1}$	20	[11]
Mn_3V_{19}	190.1	100 $mA\ g^{-1}$	100	[12]
γ -LiV_2O_5	220	50 $mA\ g^{-1}$	20	[13]
$Li_7[V_{15}O_{36}(CO_3)]$	140	2 $A\ g^{-1}$	100	[14]
$K_7NiV_{13}O_{38}$	200	17 $mA\ g^{-1}$	24	[15]
$K_3[PMo_{12}O_{40}]$	200	50 μA	10	[15]
$TBA_3[PMo_{12}O_{40}]$	260	1 mA	10	[16]
$TBA_3[PMo_{12}O_{40}]$/S-rGO	320	1 mA	100	[17]
$Na_2H_8[MnV_{13}O_{38}]$/G	190	0.1 C	100	[18]
$Na_2H_8[MnV_{13}O_{38}]$	100	0.1 C	100	[18]
$K_{5.72}H_{3.28}[PV_{14}O_{42}]$ (KPV)	140	100μA	50	[19]
1	97.7	2 $A\ g^{-1}$	100	This work
2	121.8	2 $A\ g^{-1}$	100	This work

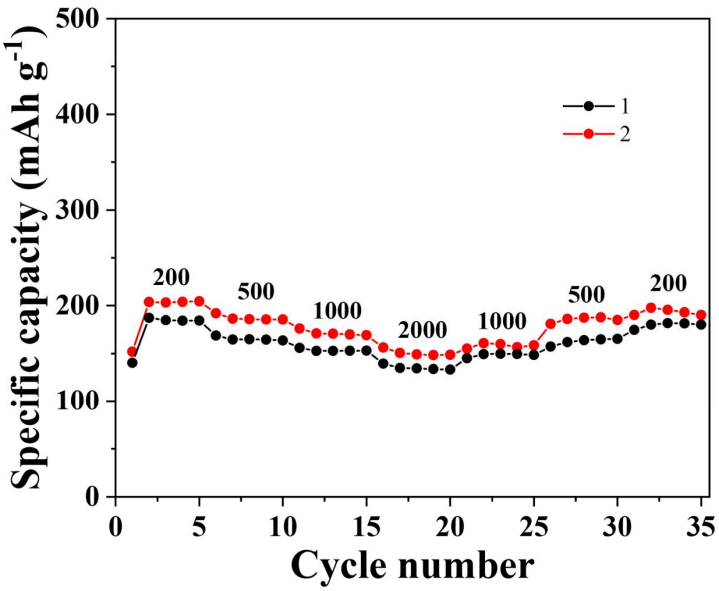

Figure S16. Rate performance of **1** and **2**.

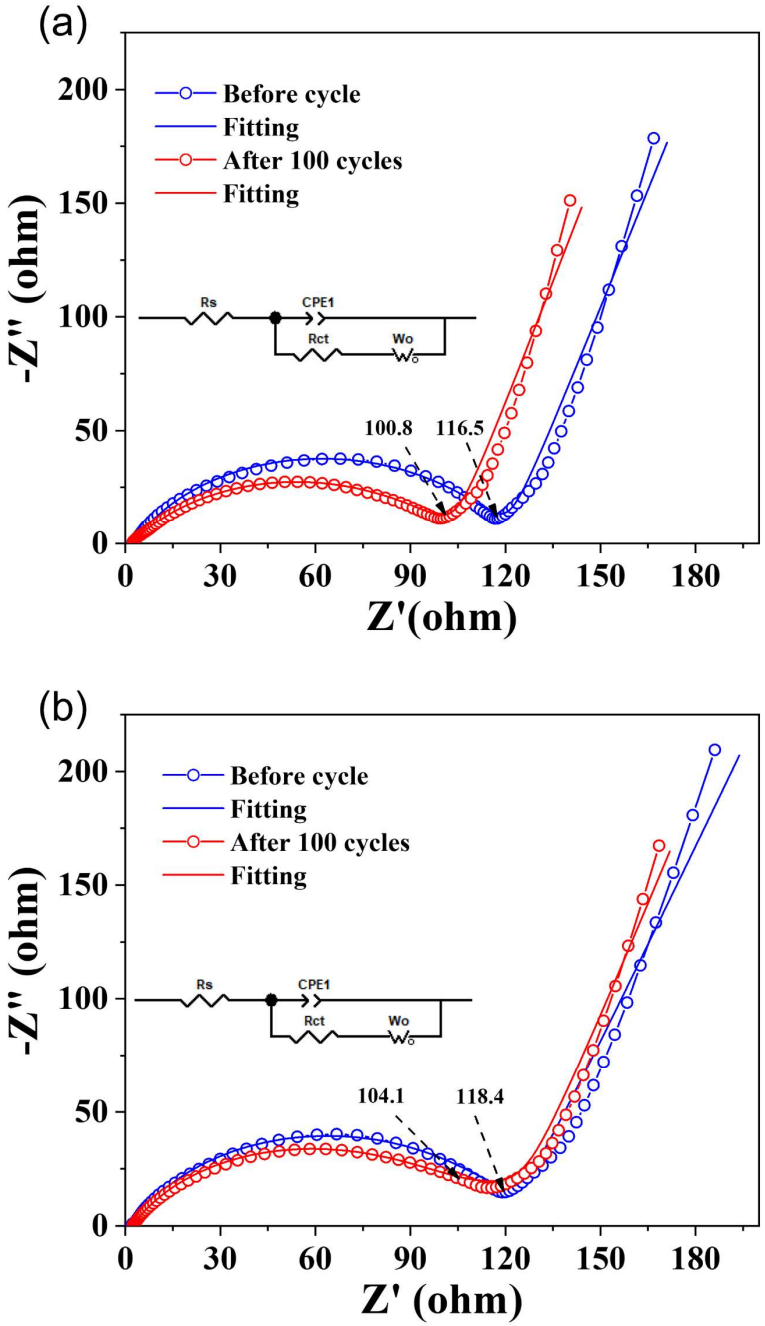

Figure S17. The Nyquist plots before cycles and after 100 charging/discharging cycles of **1** (a) and **2** (b).

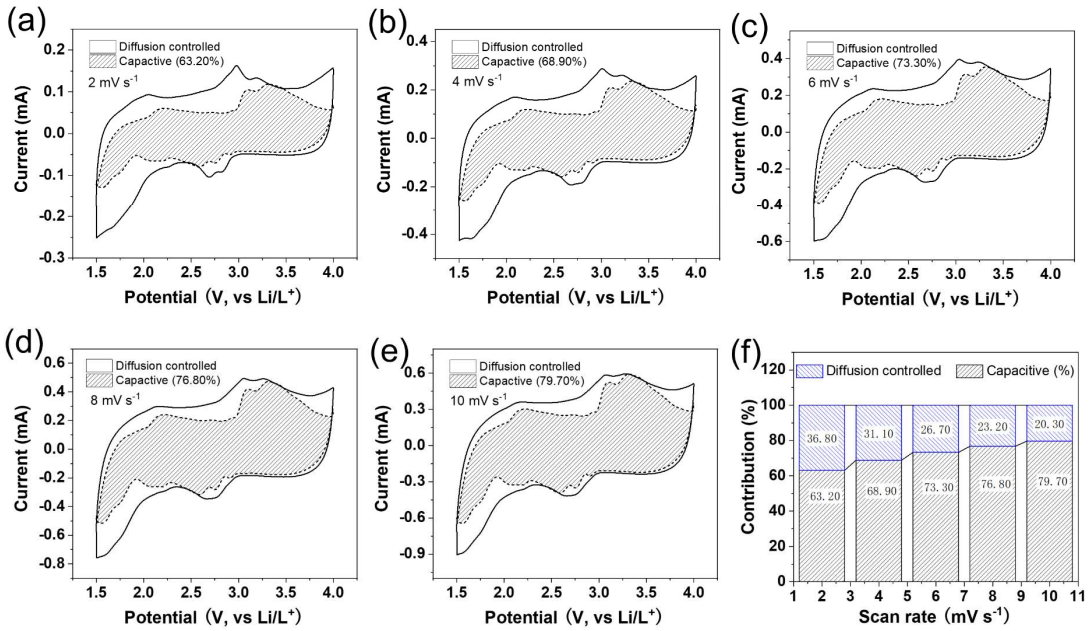

Figure S18. Capacity contribution analysis of **1** at different scan rates (2-10 mV s^{-1}).

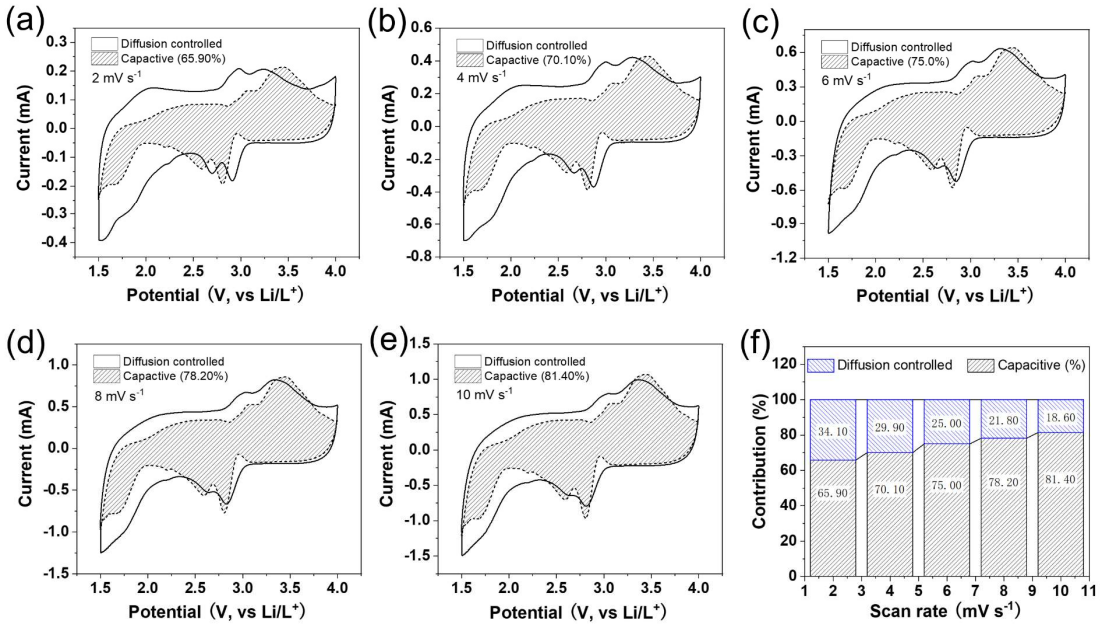

Figure S19. Capacity contribution analysis of **2** at different scan rates (2-10 mV s^{-1}).

9. The xyz coordinates of computationally studied models.

Table S8 Cartesian coordinates (in Angstroms) of the hybrid POM**1**.
$[Mo^{IV}_3Mo^{VI}_2O_{10}Sr_2(H_2O)_5(C_6H_4O_7)_2py_3]$
Level: B3LYP/Lanl2DZ
99

Mo	8.79616	8.93436	12.71551
Mo	8.15718	2.52958	12.76650
Mo	9.87574	6.83982	9.75877
Mo	9.73466	5.60765	11.93119
Mo	9.52901	4.36620	9.77777
Sr	2.78190	9.67636	12.39455
Sr	3.10719	5.38395	13.52261
O	8.27942	5.79601	10.50193
O	8.75458	7.32234	8.03541
O	8.19930	8.53728	6.30379
O	8.94799	8.61127	10.53716
O	7.61225	11.84341	9.98872
O	8.54656	4.29240	12.98135
O	10.46144	9.35192	12.86912
O	8.11916	9.47608	14.19967
O	8.83265	7.12511	12.91248
O	6.59576	8.69371	12.11204
O	7.06756	3.44530	6.45401
O	8.24678	4.28855	8.08434
O	5.47758	0.64849	10.35904
O	7.20907	0.91321	11.74732
O	9.69057	1.79147	12.74416
O	7.48888	2.04423	14.29959
O	4.68663	8.93200	11.00480
O	8.16117	2.95951	10.60534
O	5.92635	3.20125	12.48812
O	3.46533	7.87824	14.37827
O	4.12435	4.16640	11.59150
O	5.66370	6.16741	13.29496
O	10.70729	4.05030	11.23388
O	8.35149	10.77370	11.78355
O	11.05944	6.85618	11.23252
O	10.73100	5.44701	8.75027
O	0.73166	4.59930	12.59821
O	1.23973	5.84641	15.22384
O	4.99903	10.51011	13.54399
N	11.40594	8.13936	8.83393
N	11.18844	5.50073	13.62822

N	10.55822	2.64335	8.82238
C	11.83644	6.63683	14.01435
C	12.80937	6.62630	15.00227
C	13.12083	5.44076	15.62575
C	12.43958	4.27781	15.25095
C	11.50631	4.36480	14.24346
C	12.01032	9.10053	9.54880
C	13.10020	9.94976	7.63171
C	12.86467	10.02226	8.97447
C	12.49778	8.98336	6.88885
C	6.65523	8.89084	9.70138
C	5.92546	8.84294	11.02114
C	7.50400	3.34388	7.61128
C	7.19732	2.16099	8.47850
C	6.96608	2.51286	9.95787
C	6.50692	1.24795	10.70081
C	5.85953	3.56972	10.10671
C	5.25052	3.66185	11.48308
C	8.01903	10.82086	10.54137
C	10.91029	2.70019	7.52150
C	11.65631	8.06122	7.50540
C	11.45143	0.43514	8.93780
C	11.81001	0.48435	7.59900
C	11.52074	1.63493	6.88738
C	8.59727	9.70917	8.35694
C	8.49912	8.47304	7.50433
C	10.83378	1.52672	9.51177
C	8.08372	9.47146	9.79045
H	6.23497	4.45432	9.86873
H	8.00882	1.76535	8.41638
H	6.42846	1.75569	8.21798
H	11.61482	7.45953	13.59420
H	13.25567	7.42886	15.24564
H	6.04357	7.00523	13.19407
H	6.23595	5.43541	13.32702
H	13.78860	5.41197	16.30085
H	12.61669	3.44938	15.68089
H	11.06415	3.56898	13.97201
H	11.84499	9.14913	10.48305
H	13.68424	10.57369	7.21691
H	13.27995	10.69317	9.50356
H	12.65049	8.93750	5.95233
H	6.12858	9.43856	9.06675
H	6.70756	7.97314	9.33370

H	5.14053	3.36636	9.45727
H	10.73403	3.49294	7.02856
H	11.25459	7.37170	6.98994
H	11.62932	-0.34221	9.45411
H	12.24234	-0.25172	7.18210
H	11.74123	1.69253	5.96512
H	8.06938	10.43490	7.93891
H	9.54175	10.00350	8.39484
H	10.59456	1.48591	10.43026
H	0.01807	4.71467	13.21487
H	0.44451	4.66568	11.69426
H	0.39800	5.74025	14.79698
H	1.24432	5.48904	16.10711
H	5.01630	10.24293	14.45185
H	5.25280	11.41734	13.42208
H	2.96026	7.95852	15.17814
H	4.37398	8.14142	14.49985

Table S9 Cartesian coordinates (in Angstroms) of the hybrid POM**2**.

$[Mo^{IV}_3Mo^{VI}_2O_{10}Sr(H_2O)_3(C_6H_4O_7)_2py_3]^{2-}$

Level: B3LYP/Lanl2DZ

86

Mo	5.62991	11.28919	2.27870
Mo	6.10468	14.61888	3.42582
Mo	7.60260	8.39362	2.92784
Mo	3.40259	11.96747	3.20853
Mo	3.99740	9.53170	2.98374
Sr	6.47243	10.96206	9.17888
O	7.30998	9.76998	7.15119
O	2.24923	7.39622	6.22308
O	4.22649	12.47130	1.57799
O	7.45450	6.51448	3.89624
O	4.90059	9.74430	1.34404
O	7.87782	8.89720	5.20388
O	4.88512	10.95335	4.16146
O	2.25628	11.92210	4.98068
O	2.39232	10.48228	2.50847
O	7.28981	10.19315	2.76709
O	9.32607	8.26634	2.93513
O	5.54265	8.21368	3.68186
O	3.86544	11.39853	8.73107
O	6.58356	13.90719	5.54463
O	2.96500	8.77295	4.66677
O	5.44406	11.79621	11.28938
O	7.73522	9.61154	10.95931

O	6.44830	12.87568	7.49566
O	7.60732	15.45392	3.58328
O	7.16617	7.77002	1.40827
O	6.61010	12.92902	2.94454
O	0.61485	12.67829	6.26846
O	4.17111	13.78071	4.09228
O	3.76945	16.54935	6.25354
O	6.67794	5.53373	5.72066
O	5.15227	16.10176	4.59917
O	5.45354	15.23982	1.96999
N	1.68051	13.18828	2.44840
N	6.66300	11.63726	0.32007
N	3.05900	7.81605	1.89258
C	7.04508	9.05747	6.14282
C	2.23451	14.27240	5.50501
C	6.61781	6.41118	4.86031
C	1.63731	12.87214	5.59932
C	1.76465	7.49908	2.08420
C	7.73523	13.09672	-1.22675
C	7.51549	10.80069	-1.75139
C	1.88553	14.33606	1.77914
C	5.48486	7.45995	4.89385
C	3.73236	7.15247	0.92784
C	4.22794	15.76673	5.43244
C	0.41666	12.74190	2.61759
C	0.83215	15.04618	1.21777
C	7.95268	12.04724	-2.11255
C	4.14990	6.70959	4.99431
C	-0.44898	14.58293	1.36681
C	-0.67634	13.40742	2.09528
C	3.03687	7.66609	5.32279
C	3.75955	14.30210	5.35785
C	5.91298	13.41505	6.52481
C	5.69950	8.37955	6.09990
C	6.89432	10.62137	-0.52333
C	1.80162	5.85407	0.35656
C	7.06638	12.86644	-0.04849
C	4.40838	13.53237	6.51427
C	1.11561	6.52846	1.33478
C	3.13714	6.16434	0.14652
H	1.98493	14.77856	6.31841
H	1.83234	14.73655	4.72853
H	1.27703	7.95758	2.75838
H	8.04772	13.96931	-1.43514

H	7.63667	10.06323	-2.33788
H	2.77067	14.66883	1.68815
H	4.64528	7.36740	0.77653
H	0.27437	11.94350	3.11236
H	0.99843	15.84682	0.73422
H	8.39116	12.19057	-2.94302
H	3.95706	6.25858	4.13437
H	4.21078	6.01659	5.69868
H	-1.17694	15.05472	0.97954
H	-1.55737	13.07716	2.22646
H	4.99539	9.07547	6.09553
H	5.58787	7.84686	6.92688
H	6.62309	9.74652	-0.27117
H	1.37070	5.18817	-0.16631
H	6.88255	13.60074	0.52555
H	4.13169	13.96557	7.36038
H	4.03240	12.61656	6.51819
H	0.20068	6.33179	1.49821
H	3.63854	5.70982	-0.52021

Table S10 Cartesian coordinates (in Angstroms) of the $[Mo_3O_4(C_2O_4)_3(Mepy)_3]^{2-}$.

$[Mo_3O_4(C_2O_4)_3(Mepy)_3]^{2-}$

Level: B3LYP/Lanl2DZ

67

Mo	3.07379	0.33549	4.28070
Mo	4.59712	-1.58878	3.83855
Mo	3.15235	-1.57466	5.88551
N	1.50931	1.21460	2.95331
N	1.58668	-2.94793	6.65599
N	4.79270	-2.97746	2.11445
O	1.65539	-0.68848	5.07031
O	3.34113	-0.72433	2.70259
O	4.65271	-0.28678	5.41094
O	4.29047	1.91679	3.63221
O	2.75107	1.86934	5.68600
O	3.46421	-2.95215	4.57379
O	3.00909	-0.60203	7.71908
O	4.51851	-2.58840	7.14440
O	6.39085	-2.41971	4.55521
O	6.12508	-0.48289	2.89885
O	5.23963	3.82831	4.25196
O	3.67273	3.72393	6.55198
O	5.67379	-2.42182	9.04891
O	3.89114	-0.37007	9.76113
O	8.29629	-0.05904	2.81684

O	8.58647	-2.06440	4.77347
C	3.57713	2.86886	5.69348
C	4.47269	2.90682	4.42707
C	3.83971	-0.89513	8.65767
C	4.79108	-2.05280	8.29249
C	7.50307	-1.81557	4.29680
C	7.33671	-0.66423	3.25677
C	0.21483	1.23463	3.25976
C	1.85812	1.50454	1.69139
C	1.77318	-4.27429	6.66880
C	0.36215	-2.48824	6.96244
C	4.70989	-2.52725	0.86278
C	4.77103	-4.30487	2.30430
C	0.94233	1.77551	0.72183
C	-0.40512	1.75337	1.01227
C	-0.75854	1.50560	2.33420
C	-1.45138	1.96740	-0.05553
C	-0.68916	-3.31695	7.26228
C	-0.50834	-4.68970	7.27168
C	0.75728	-5.15994	6.97056
C	-1.66549	-5.61752	7.53649
C	4.52120	-3.36756	-0.20075
C	4.42129	-4.74348	0.01068
C	4.58898	-5.20528	1.29203
C	4.08765	-5.70082	-1.11905
H	2.76055	1.52036	1.46928
H	1.22662	1.97689	-0.14095
H	-1.65122	1.52458	2.58833
H	-0.03995	1.05750	4.13663
H	-2.24443	1.47502	0.17085
H	-1.11321	1.66269	-0.89908
H	-1.66078	2.90260	-0.11319
H	0.22060	-1.56886	6.97056
H	-1.52380	-2.95742	7.45961
H	0.92335	-6.07511	6.97270
H	2.61721	-4.60957	6.46656
H	-1.77995	-5.72085	8.48469
H	-1.48818	-6.47365	7.14141
H	-2.46450	-5.24850	7.15636
H	4.78115	-1.61314	0.70688
H	4.46090	-3.02279	-1.06352
H	4.57903	-6.11728	1.46928
H	4.88482	-4.62961	3.16921
H	4.45229	-6.56748	-0.92257

H	4.46581	-5.37292	-1.93698
H	3.13573	-5.76724	-1.21088

Table S11 Cartesian coordinates (in Angstroms) of the $[Mo^{IV}_3Mo^{VI}_2O_{10}(C_6H_4O_7)_2py_3]^{4-}$.

$[Mo^{IV}_3Mo^{VI}_2O_{10}(C_6H_4O_7)_2py_3]^{4-}$

Level: B3LYP/Lanl2DZ

82

Mo	5.62960	11.28918	2.27878
Mo	3.99732	9.53173	2.98346
Mo	3.40248	11.96765	3.20837
Mo	6.10458	14.61879	3.42581
Mo	7.60255	8.39311	2.92806
N	6.65903	11.64054	0.32313
N	1.68092	13.18306	2.44496
N	3.06046	7.81391	1.89102
O	4.90058	9.74540	1.34457
O	4.22810	12.47014	1.58063
O	6.61100	12.92776	2.94318
O	7.28862	10.19167	2.76904
O	4.88277	10.95141	4.15930
O	2.39514	10.48091	2.50943
O	2.25671	11.92318	4.97906
O	4.17150	13.77828	4.09212
O	2.96506	8.77416	4.66516
O	5.54203	8.21229	3.68368
O	5.45339	15.23935	1.96743
O	7.60551	15.45214	3.58148
O	5.15156	16.10111	4.60181
O	6.58353	13.90635	5.54255
O	7.16738	7.77014	1.40872
O	9.32598	8.26720	2.93682
O	7.45270	6.51358	3.89188
O	7.87893	8.89769	5.20302
O	7.31059	9.76840	7.15023
O	6.44906	12.87745	7.49565
O	0.61452	12.68164	6.26680
O	3.76660	16.54891	6.25248
O	2.24738	7.39832	6.22064
O	6.67852	5.53393	5.72242
C	3.76188	14.30156	5.35472
C	1.63766	12.87510	5.59667
C	4.22742	15.76948	5.43431
C	5.91352	13.41998	6.52626
C	5.48283	7.46254	4.89469
C	3.03497	7.66208	5.31970

C	6.61600	6.40603	4.85968
C	7.04384	9.06025	6.14742
C	6.89403	10.62242	-0.52528
C	7.07084	12.86810	-0.04457
C	1.88484	14.33605	1.78119
C	0.41931	12.73875	2.61687
C	3.72872	7.15119	0.92641
C	1.76445	7.49570	2.08363
C	7.73632	13.09443	-1.22885
C	7.95266	12.04897	-2.11228
C	7.51961	10.79872	-1.74776
C	0.83949	15.05572	1.22248
C	-0.45540	14.57335	1.36733
C	-0.67585	13.40845	2.09159
C	1.11484	6.52554	1.33550
C	1.80243	5.85238	0.35178
C	3.14338	6.16536	0.14963
C	2.23202	14.26737	5.50434
C	4.40855	13.53101	6.51193
C	4.15015	6.71293	4.99498
C	5.69940	8.38135	6.10126
H	6.89666	13.60224	0.53156
H	8.04684	13.96717	-1.44033
H	8.38855	12.19337	-2.94415
H	7.64828	10.05964	-2.33116
H	6.61876	9.74753	-0.27577
H	2.77145	14.66720	1.69229
H	1.00484	15.86252	0.75012
H	-1.18492	15.03783	0.97493
H	-1.55656	13.07772	2.22389
H	0.27588	11.94107	3.11231
H	1.27798	7.95411	2.75868
H	0.20049	6.32671	1.50185
H	1.37194	5.19091	-0.17608
H	3.64940	5.70946	-0.51145
H	4.64114	7.36896	0.77358
H	1.98335	14.77083	6.31979
H	1.82855	14.73274	4.73031
H	4.12734	13.96133	7.35871
H	4.03563	12.61384	6.51289
H	3.95888	6.26031	4.13552
H	4.21151	6.02118	5.70007
H	4.99555	9.07771	6.09691
H	5.58749	7.84857	6.92734

Table S12 Cartesian coordinates (in Angstroms) of the $[Mo^{IV}_3Mo^{VI}_2O_{18}py_3]^{12-}$.

$[Mo^{IV}_3Mo^{VI}_2O_{18}py_3]^{12-}$

Level: B3LYP/Lanl2DZ

56

Mo	9.73474	5.60748	11.93136
Mo	9.52881	4.36655	9.77821
Mo	9.87568	6.83981	9.75880
Mo	8.79611	8.93434	12.71526
Mo	8.15726	2.52955	12.76640
N	11.18827	5.50412	13.62718
N	11.40390	8.14203	8.83636
N	10.55859	2.64104	8.82367
O	11.05944	6.85826	11.23105
O	10.70556	4.04834	11.23431
O	8.83279	7.12408	12.91219
O	8.28126	5.79809	10.50191
O	8.54437	4.29446	12.98091
O	10.73587	5.44501	8.74950
O	8.75690	7.32486	8.03632
O	8.94720	8.60957	10.53745
O	8.24785	4.28758	8.08347
O	8.16276	2.95846	10.60527
O	8.11533	9.47271	14.19875
O	10.46206	9.35075	12.86921
O	8.35379	10.77525	11.78176
O	6.59468	8.69401	12.11342
O	9.69117	1.79197	12.74445
O	7.48803	2.04215	14.30084
O	7.20896	0.91193	11.74730
O	5.92669	3.19927	12.48660
C	11.50317	4.36577	14.24372
C	11.83759	6.63465	14.01342
C	12.01239	9.09900	9.54175
C	11.66332	8.06697	7.50356
C	10.82994	1.52614	9.50911
C	10.90530	2.70515	7.52170
C	12.80951	6.62683	14.99625
C	13.12538	5.43688	15.62547
C	12.44696	4.28133	15.25012
C	12.85995	10.02000	8.97055
C	13.10606	9.95120	7.62324
C	12.49246	8.98016	6.88703
C	11.52138	1.64185	6.88522
C	11.80857	0.48943	7.60330

C	11.45085	0.43939	8.93610
H	11.61516	7.45722	13.59333
H	13.25793	7.42950	15.23450
H	13.79029	5.40994	16.30286
H	12.63029	3.45299	15.67657
H	11.05698	3.56992	13.97625
H	11.85349	9.14677	10.47804
H	13.26785	10.69378	9.50091
H	13.69592	10.56924	7.20988
H	12.63584	8.93408	5.94961
H	11.26803	7.37392	6.98867
H	10.72341	3.49679	7.02960
H	11.74538	1.69910	5.96403
H	12.24271	-0.24704	7.18843
H	11.62945	-0.33736	9.45291
H	10.58350	1.48319	10.42615

References

1 A. Bino, F. A. Cotton and Z. Dori, *J. Am. Chem. Soc.*, 1978, **100**, 5252-5253.

2 S. F. Gheller, T. W. Hambley, R. T. C. Brownlee, M. J. O'Connor, M. R. Snow and A. G. Wedd, *J. Am. Chem. Soc.*, 1983, **105**, 1527-1532.

3 A. Birnbaum, F. A. Cotton, Z. Dori, D. O. Marler, G. M. Reisner, W. Schwotzer and M. Shaia, *Inorg. Chem.*, 1983, **22**, 2723-2726.

4 G. M. Sheldrick, *Acta Crystallogr. A*, 2015, **71**, 3-8.

5 R. Tsunashima, Y. Iwamoto, Y. Baba, C. Kato, K. Ichihashi, S. Nishihara, K. Inoue, K. Ishiguro, Y. F. Song and T. Akutagawa, *Angew. Chem. Int. Ed.*, 2014, **53**, 11228-11231.

6 A. D. Becke, *J. Chem. Phys.*, 1993, **98**, 5648-5652.

7 Gaussian 16, Revision A. 03, M. J. Frisch, G. W. Trucks, H. B. Schlegel, G. E. Scuseria, M. A. Robb, J. R. Cheeseman, V. B. G. Scalmani, G. A. Petersson, H. Nakatsuji, X. Li, M. Caricato, A. V. Marenich, J. Bloino, B. G. Janesko, R. Gomperts, B. Mennucci, H. P. Hratchian, J. V. Ortiz, A. F. Izmaylov, J. L. Sonnenberg, D. Williams-Young, F. Ding, F. Lipparini, F. Egidi, J. Goings, B. Peng, A. Petrone, T. Henderson, D. Ranasinghe, V. G. Zakrzewski, N. R. J. Gao, G. Zheng, W. Liang, M. Hada, M. Ehara, K. Toyota, R. Fukuda, J. Hasegawa, M. Ishida, T. Nakajima, Y. Honda, O. Kitao, H. Nakai, T. Vreven, K. Throssell, J. A. Montgomery, J. E. P. Jr., F. Ogliaro, M. J. Bearpark, J. J. Heyd, E. N. Brothers, K. N. Kudin, V. N. Staroverov, R. K. T. A. Keith, J. Normand, , K. Raghavachari, A. P. Rendell, J. C. Burant, S. S. Iyengar, J. Tomasi, M. Cossi, J. M. Millam, M. Klene, C. Adamo, R. Cammi, J. W. Ochterski, R. L. Martin, K. Morokuma, O. Farkas, J. B. Foresman and and D. J. Fox, 2016.

8 P. J. Stephens, F. J. Devlin, C. F. Chabalowski and M. J. Frisch, *J. Phys. Chem.*, 1994, **98**, 11623-11627.

9 P. J. Hay and W. R. Wadt, *J. Chem. Phys.*, 1985, **82**, 270-283.

10 M. M. Francl, W. J. Pietro, W. J. Hehre, J. S. Binkley, M. S. Gordon, D. J. Defrees and J. A. Pople, *J. Chem. Phys.*, 1982, **77**, 3654-3665.

11 S. Wang, H. L. Li, S. Li, F. Liu, D. Q. Wu, X. L. Feng and L. X. Wu, *Chem.-Eur. J.*, 2013, **19**, 10895-10902.

12 F. C. Shen, Y. R. Wang, S. L. Li, J. Liu, L. Z. Dong, T. Wei, Y. C. Cui, X. L. Wu, Y. Xu and Y. Q. Lan, *J. Mater. Chem. A*, 2018, **6**, 1743-1750.

13 H. Wang, J. Isobe, T. Shimizu, D. Matsumura, T. Ina and H. Yoshikawa, *J. Power Sources*, 2017, **360**, 150-156.

14 J. J. Chen, M. D. Symes, S. C. Fan, M. S. Zheng, H. N. Miras, Q. F. Dong and L. Cronin, *Adv. Mater.*, 2015, **27**, 4649-4654.

15 N. Sonoyama, Y. Suganuma, T. Kume and Z. Quan, *J. Power Sources*, 2011, **196**, 6822-6827.

16 H. Wang, S. Hamanaka, Y. Nishimoto, S. Irle, T. Yokoyama, H. Yoshikawa and K. Awaga, *J. Am. Chem. Soc.*, 2012, **134**, 4918-4924.

17 H. Omachi, T. Inoue, S. Hatao, H. Shinohara, A. Criado, H. Yoshikawa, Z. Syrgiannis and M. Prato, *Angew. Chem. Int. Edit.*, 2020, **59**, 7836-7841.

18 J. L. Liu, Z. Chen, S. Chen, B. W. Zhang, J. Wang, H. H. Wang, B. B. Tian, M. H. Chen, X. F. Fan, Y. Z. Huang, T. C. Sum, J. Y. Lin and Z. X. Shen, *ACS Nano*, 2017, **11**, 6911-6920.

19 S. Uematsu, Z. Quan, Y. Suganuma and N. Sonoyama, *J. Power Sources*, 2012, **217**, 13-20.